

Thermoelectric properties of $\text{Sm}_3\text{Rh}_4\text{Ge}_{13}$

S P Xhakaza¹, B M Sondezi¹ and A M Strydom¹

¹Highly Correlated Matter Research Group, Physics Department, University of Johannesburg, P. O. Box 524, Auckland Park 2006, South Africa

E-mail: psindisiwe@gmail.com

Abstract. We report the first results on thermoelectric properties of the cubic intermetallic compound $\text{Sm}_3\text{Rh}_4\text{Ge}_{13}$. The compound displays semiconductor-like behaviour with high resistivity $\rho(T)$ values and a negative temperature coefficient in $\rho(T)$ throughout the entire temperature range investigated. The thermal conductivity, $\kappa_T(T)$ observed in $\text{Sm}_3\text{Rh}_4\text{Ge}_{13}$ is extremely low and only weakly temperature dependent. A high thermopower amounting to $34 \mu\text{V}\cdot\text{K}^{-1}$ is observed at room temperature. We discuss the origins of a low charge carrier density and anharmonic lattice vibration modes in this cage-type system.

1. Introduction

Thermoelectricity is a general phenomenon that can be seen in electrically conductive materials due to heat transport by charge carriers and scattering processes between charge carriers. Materials of high thermoelectric merit are capable of converting waste heat to useful electricity and *vice versa*. Therefore, applications in clean energy is a key reason for studying thermoelectricity [1]. This has motivated researchers to search for new and more efficient thermoelectric materials. The efficiency of the material is determined by the dimensionless thermoelectric figure of merit $zT = S^2T/(\rho\kappa)$, in terms of the Seebeck coefficient (thermopower) S , electrical resistivity ρ and thermal conductivity κ . Samarium is one of the elements that has received comparably less attention in the family of ternary intermetallic compounds of composition $R_3X_4\text{Ge}_{13}$ (R = rare-earth element and X = d-electron element), especially in thermal transport properties. Sm-based compounds occasionally exhibit heavy-fermion or strongly correlated electron features which is an aspect that will make this study of particular interest in the correlated electron and quantum matter communities.

The CoSb_3 skutterudite structure in particular has been of much interest and it contains two large empty cages per unit cell, filling the empty cages with rare-earth atoms resulting in an enhanced thermoelectric figure of merit [2]. Upon substitution of the rare-earth element, $\text{Sm}_{0.6}\text{Co}_4\text{Sb}_{12}$ for example achieved a maximum value $zT = 0.8$ at $716 \text{ }^\circ\text{C}$ [3]. The existence of $\text{Sm}_3\text{Rh}_4\text{Ge}_{13}$ has been reported by Venturini *et al.* [4], among thirty-four new ternary germanide compounds of composition $R_3T_4\text{Ge}_{13}$. Among these germanides interesting physics have been studied. Kong *et al.* [5] reported thermoelectric properties of $R_3\text{Ru}_4\text{Ge}_{13}$ ($R = \text{Y, Dy, Ho and Lu}$) in which high thermopower values were observed at room temperature with very low thermal conductivity, however these materials did not display very high figure of merit values $R_3X_4A_{13}$ (R = rare-earth, X = d-electron element, A = p-electron element) crystallizes in a cubic space group $Pm\bar{3}n$, involving two formula units per unit cell. The development of $R_3X_4A_{13}$ phases is credited to Remeika *et al.* [6]. In this paper, we explore thermoelectric properties of $\text{Sm}_3\text{Rh}_4\text{Ge}_{13}$.

2. Experimental method

A polycrystalline sample of $\text{Sm}_3\text{Rh}_4\text{Ge}_{13}$ was prepared by arc-melting high-purity elemental constituents of Sm (4N), Rh (4N) and Ge (5N). The stoichiometric ratio of the elements was melted using an Edmund Buehler arc-furnace under an atmosphere of purified Argon gas. The melted sample was overturned and melted five times to ensure good homogeneity. The sample was then wrapped in tantalum foil and set for annealing in an evacuated quartz tube for 5 days at 700 °C followed by further annealing for 7 days at 900 °C. Powder x-ray diffraction (XRD) patterns were obtained in a Rigaku SmartLab diffractometer using Cu-K α 1 radiation. The phase analysis was carried out by simulating the obtained experimental powder pattern with theoretical calculated patterns using Powder-Cell [7]. The powder diffractogram showed good agreement with the expected $Pm\bar{3}n$ space group. A structural survey of a piece of the sample was performed using GSAS software. The Rietveld fit (red line) and experimental data (circle symbol) with expected Bragg positions as vertical lines are shown in figure 1. The value of the lattice parameter estimated from the fit was $a = 0.8978(5)$ nm in close agreement with the previously reported value [4] of $a = 0.8984(7)$ nm.

The sample was cut into geometries appropriate for various measurements. Physical properties comprising electrical resistivity, thermal conductivity and thermopower were studied on a Physical Properties Measurement System (PPMS) from Quantum Design (San Diego), using the thermal transport platform. All measurements were conducted from room temperature down to 2 K.

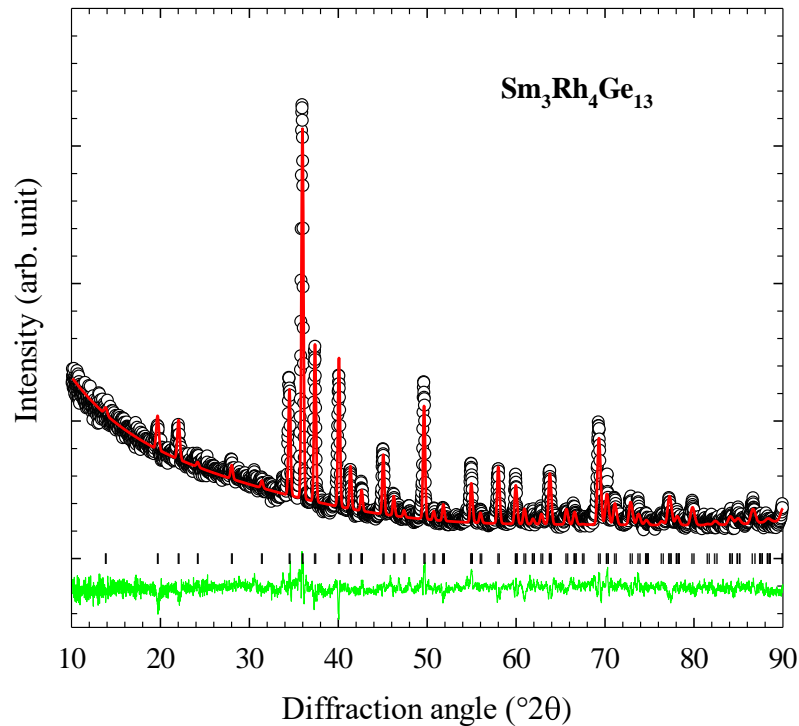


Figure 1: Experimental powder X-ray pattern of $\text{Sm}_3\text{Rh}_4\text{Ge}_{13}$ (circle symbol), Rietveld refinement fit (red line), difference curve (green line) and expected Bragg positions (vertical marks).

3. Results and discussion

3.1. Electrical transport

The temperature dependence of resistivity, $\rho(T)$ of $\text{Sm}_3\text{Rh}_4\text{Ge}_{13}$ is presented in the main panel of figure 2. In general, a semiconductor-like behavior is observed. The overall $\rho(T)$ values are ~ 100 times greater than in ordinary metals, and moreover $\rho(T)$ increases with decrease in temperature through the entire range. Similar behavior was observed in superconducting non-magnetic compounds $\text{Y}_3\text{X}_4\text{Ge}_{13}$ ($X = \text{Rh, Ir, Os}$) and $\text{Lu}_3\text{X}_4\text{Ge}_{13}$ ($X = \text{Rh, Co, Os}$) [8, 9, 10]. This trend of semiconducting behavior is also observed in a range of similar magnetic $\text{R}_3\text{Ru}_4\text{Ge}_{13}$ compounds having $R = \text{Sm, Nd, Dy, Ho}$ and Er [5, 11, 13] as well as $\text{Yb}_3\text{Ir}_4\text{Ge}_{13}$ [12]. No phase transition is observed in $\rho(T)$ anywhere in $\text{Sm}_3\text{Rh}_4\text{Ge}_{13}$ in figure 2 and we furthermore note that $\rho(T)$ increases unabatedly towards $T \rightarrow 0$. As a first observation we note that the presence of a magnetic ion R in $\text{R}_3\text{X}_4\text{Ge}_{13}$ is not directly connected to semiconducting behavior as $\text{Y}_3\text{Rh}_4\text{Ge}_{13}$ [8] displays similar behavior. Further, germanium may at first sight be attributed to the prevalence of semiconducting behavior in these compounds on account of the presence of 65 % atomic percentage of Ge in the formula, but semiconductivity is not ubiquitous among the germanides. We note for instance the case of $\text{Yb}_3\text{Co}_4\text{Ge}_{13}$ with weak metallic behavior and $\text{Yb}_3\text{Rh}_4\text{Ge}_{13}$ which shows a well-defined metallic electrical resistivity [8, 12]. An activated type of resistivity has been observed in many of $\text{R}_3\text{X}_4\text{A}_{13}$ systems [13]. In order to analyze the electrical resistivity the high temperature region was described (see fit in inset of figure 2) in terms of simple energy gap by the expression $\rho(T) = C \exp(-T/\Delta)$ with $C = 5400 \mu\Omega\cdot\text{cm}$ and the energy gap value $\Delta = 158.7 \text{ K}$.

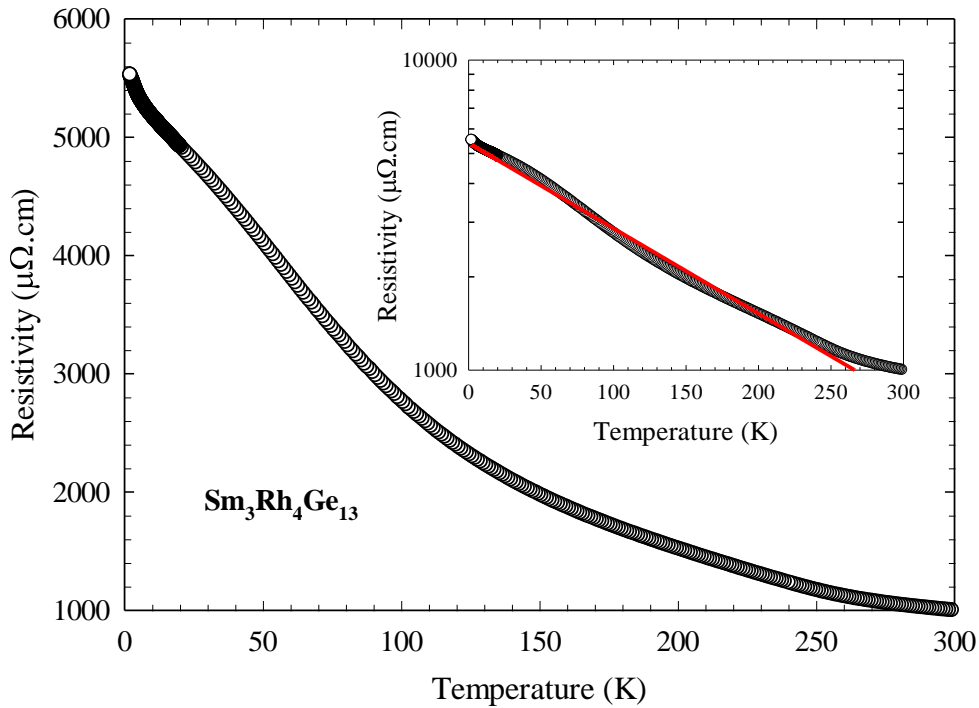


Figure 2: The electrical resistivity as a function of temperature plotted in the main panel. Inset: $\rho(T)$ on a semi-log axis where the solid line is an exponential fit in terms of a single energy gap.

3.2. Thermal transport

The thermal transport in $\text{Sm}_3\text{Rh}_4\text{Ge}_{13}$, including total thermal conductivity $\kappa_T(T)$, electrical resistivity $\rho(T)$ and thermopower $S(T)$ were all measured concurrently using a thermal transport measurement platform in the PPMS cryogenic facility. The temperature dependence of $\kappa_T(T)$ was measured upon cooling down very slowly under quasi-adiabatic conditions from room temperature

to 2 K with results as shown in figure 3a using open circles. We note that $\kappa_T(T)$ is overall extremely low, by more than an order of magnitude as compared to thermal conductivity in ordinary metals. The thermal conductivity bears a resemblance to that of $\text{Sm}_3\text{Ru}_4\text{Ge}_{13}$ [11] and to many skutterudites, a structure type that is recognized as a promising materials class for developing novel thermoelectric materials [14, 15].

The electronic contribution $\kappa_e(T)$ to total thermal conductivity $\kappa_T(T)$ was extracted by means of the Wiedemann-Franz relation;

$$\kappa_e(T) = \frac{L_0 T}{\rho(T)} \quad (1)$$

where the Lorenz number is $L_0 = 2.44 \times 10^{-8} \text{ W}\Omega\cdot\text{K}^{-2}$. The lattice (phononic) thermal conductivity $\kappa_L(T)$ contribution to total thermal conductivity was extracted by using the expression:

$$\kappa_T(T) = \kappa_L(T) + \kappa_e(T). \quad (2)$$

This expression assumes that possible contributions to κ_T from magnon heat transport are ignored. The estimated $\kappa_e(T)$ contribution is smaller than that of the lattice conductivity by more than two orders of magnitude compared to the total thermal conductivity contribution as shown in figure 3a using red closed circle symbols. Such conductivity behaviour suggests that heat is carried by phonons much more efficiently than by electrons. From figure 3a, we can thus approximate the lattice to $\kappa_L(T) \simeq \kappa_T(T)$. A weak plateau above $T \sim 50$ K is evident in $\kappa_T(T)$ between 10 K and 200 K which signifies glassy behaviour in the thermal conductivity and is likely the result of optical (anharmonic phonon) modes produced by the cage-like structure of $\text{Sm}_3\text{Rh}_4\text{Ge}_{13}$ [9]. Below 10 K the electronic contribution produces a $\kappa_e(T) \sim T$ dependence which is typical for metallic behaviour and above 100 K electronic contribution produces a $\kappa_e(T) \sim T^2$ dependence.

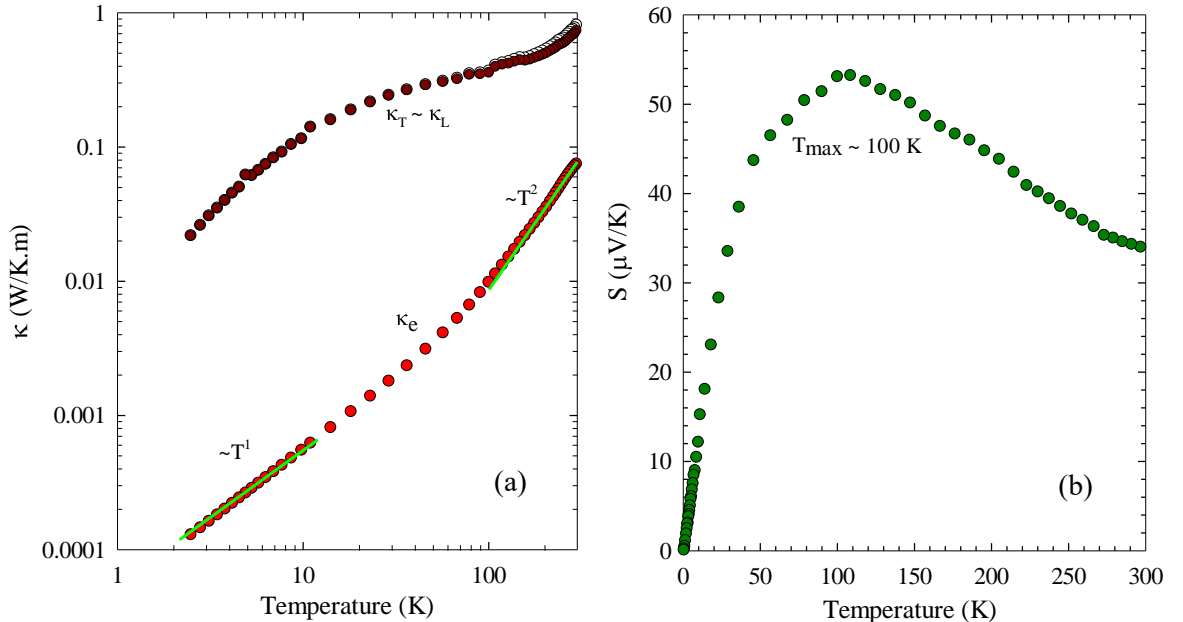


Figure 3: (a) Temperature dependence of the total thermal conductivity $\kappa_T(T)$ of $\text{Sm}_3\text{Rh}_4\text{Ge}_{13}$ plotted in log-log scale along with the electronic contribution, $\kappa_e(T)$ and lattice contribution $\kappa_L(T)$. The Seebeck coefficient, S is plotted in (b) and displays a maximum at $T_{\max} = 100$ K.

The thermopower shown in figure 3b reaches the value of $34 \mu\text{V.K}^{-1}$ at room temperature. This value is in between that of metals ($\sim 1 - 10 \mu\text{V.K}^{-1}$) and semiconductors ($\sim 10^2 - 10^3 \mu\text{V.K}^{-1}$). The value of thermopower is related to that of $\text{Y}_3\text{Ir}_4\text{Ge}_{13}$ and $\text{R}_3\text{Ru}_4\text{Ge}_{13}$ ($R = \text{Sm, Y, Dy, Ho and Lu}$) [5, 9, 11]. A positive thermopower $S(T)$, peak in $S(T)$ at $T_{\text{max}} \sim 100 \text{ K}$, quasi-exponential $\rho(T)$ and $\rho(T)$ energy gap of $\sim 158 \text{ K}$ all support consistently that this is a narrow-gap activated semiconducting system, with gapping at the Fermi energy responsible for all the anomalous thermal and electronic transport behaviours.

4. Conclusions

We have reported on findings of a thermoelectric study on $\text{Sm}_3\text{Rh}_4\text{Ge}_{13}$. Structural analysis of the x-ray diffraction confirms the compound to adopt the cubic space group $Pm\bar{3}n$. The thermal transport exhibits only weak temperature dependence in thermal conductivity below room temperature and 2 K. The thermopower reaches fairly high and positive values which resembles a hole-dominated character near the Fermi surface as is also supported by the activated type behavior found in the electrical resistivity.

Acknowledgements

SPX acknowledges the Faculty of Science at UJ and the SA-NRF Scarce Skills Development Funds master's degree scholarship and research group of Highly Correlated Matter Physics for their endless support. BMS acknowledges NRF-Thuthuka grant (99231) and AMS thanks the SA-NRF and the FRC/URC of UJ for financial assistance.

References

- [1] Zlatic V and Hewson A 2011 *New Material for Thermoelectric Applications* (Springer)
- [2] Meinser G P, Morelli D T, Hu S, Yang J and Uher C 1998 *Phys. Rev. Lett.* **80** 3551
- [3] Zhang Q, Chen C, Kang Y, Li X, Zhang L, Yu D, Tian Y and Xu B 2015 *Mater. Lett.* **143** 41-3
- [4] Venturini G, Méot-Mayer M, Malaman B and Roques B 1985 *J. Less-Common Met.* **113** 197
- [5] Kong H, Shi X, Uher C and Morelli D T 2007 *J. Appl. Phys.* **102** 023702
- [6] Remeika J P *et al* 1980 *Solid State Commun.* **34** 923-26
- [7] Krauss W and Nolze G 1996 *J. Appl. Cryst.* **29** 301
- [8] Strydom A M 2014 *Acta. Phys. Polon. A.* **126** 319-20
- [9] Strydom A M 2007 *J. Phys.: Condens. Matter.* **19** 386205
- [10] Rai B K, Oswald I H W, Wang J K, McCandless G T, Chan J Y and Marosan E 2015 *Chem. Mater.* **27** 2488
- [11] Nair H S, Kumar R, Britz D, Ghosh S K, Reinke C and Strydom A M 2016 *J. Alloys. Comp.* **669** 254-61
- [12] Rai B K, Oswald I H W, Chan J Y and Morosan E 2016 *Phys. Rev. B.* **93** 035101
- [13] Ghosh K, Ramakrishnan and Chandra G 1993 *Phys. Rev. B.* **48** 10435
- [14] Rogl G, Grytsiv A, Failamani F, Hochenhofer M, Bauer E and Rogl P 2017 *J. Alloys. Comp.* **695** 682-696
- [15] Shi X, Yang J, Salvador J R, Chi M, Cho Y Y, Wang H, Bai S, Yang J, Zhang W and Chen L 2011 *J. Am. Chem. Soc.* **133** 7837-46